International Journal of Advanced Engineering Research and Science (IJAERS)
Peer-Reviewed Journal
ISSN: 2349-6495(P) | 2456-1908(O)
Vol-13, Issue-8; Aug, 2026
Journal Home Page Available: https://ijaers.com/
Article DOI: https://dx.doi.org/10.22161/ijaers.138.4

Research on Thermal Field Prediction Method of Lithium Battery Module Based on PINN

Qiang-Sheng Xiao, Yan-Zuo Chang*, Lei Huang

School of Energy and Power Engineering, Guangdong University of Petrochemical Technology, Maoming, Guangdong 525000, China
*Corresponding author: 2943194487@qq.com

Received: 03 Jul 2026,

Received in revised form: 01 Aug 2026,

Accepted: 05 Aug 2026,

Available online: 12 Aug 2026

Keywords*— *battery thermal management, lithium battery module, multi-physics constraints, PINN, thermal field prediction

***Abstract*—** *Accurate thermal field prediction is essential for optimizing battery thermal management systems and preventing thermal runaway of lithium battery modules. Traditional thermal prediction methods, including experimental measurement, numerical simulation, and pure data-driven modeling, suffer from obvious limitations such as heavy data dependence, high computational consumption, and poor physical interpretability. To address these issues, this paper develops a multi-physics constrained three-dimensional transient thermal field prediction framework for lithium battery modules based on physics-informed neural networks. The framework integrates transient heat conduction principles and couples Joule irreversible heat and entropy reversible heat to characterize internal heat generation. On the basis of conventional thermal boundary and initial constraints, charge consistency and material interface continuity constraints are innovatively introduced to optimize the loss function, combined with efficient training optimization strategies. The results indicate that the proposed mesh-free framework can achieve high-precision full-domain thermal field reconstruction using only sparse temperature data. It strictly complies with fundamental heat transfer and charge conservation laws, adapts to complex battery module structures, and provides an effective solution for fast, accurate thermal prediction of lithium batteries under sparse sensor working conditions.*

I. INTRODUCTION

Driven by the global energy transition and the "carbon neutrality" target, lithium-ion battery energy storage technology has been widely applied in electric vehicles, grid energy storage and other fields. Nevertheless, the performance, service life and safety of lithium batteries are closely related to their actual operating temperature. A large amount of heat is generated inside batteries during charging and discharging due to electrochemical reactions and Joule effects. If heat cannot be dissipated efficiently and timely, the battery temperature will rise. When the temperature exceeds the optimal operating range (usually 20–40°C) [1], it will accelerate aging phenomena such as capacity fade and internal resistance increase. Worse still, local overheating may trigger thermal runaway, leading to catastrophic safety accidents including combustion and explosion.

In engineering applications, lithium batteries are generally integrated into modules and battery packs equipped with Battery Thermal Management System (BTMS) for temperature regulation. A well-designed BTMS can maintain the temperature of all single cells inside the module within an appropriate range and guarantee uniform temperature distribution[2]. Therefore, accurate and fast prediction of the internal three-dimensional transient thermal field of lithium battery modules under

various working conditions has become the core task of BTMS design, optimization and control, which is of vital significance for improving the overall safety, reliability and economy of battery systems.

According to existing literature, there are three mainstream methods for characterizing lithium battery thermal field prediction: experimental methods, model-based methods and data-driven methods [3]. Experimental methods feature high precision yet high cost and limited measurement points, failing to acquire full-domain temperature distribution. Numerical simulation methods (e.g., finite element method) possess clear physical mechanisms, but suffer from long modeling cycles and low computational efficiency for complex modules, making it difficult to meet real-time prediction requirements. Pure data-driven methods (e.g., BP neural networks) rely on massive labeled data[4], and suffer from poor physical consistency and weak generalization ability, which tend to generate non-physical prediction results violating heat transfer laws.

The emergence of Physics-Informed Neural Networks (PINN) provides a new approach to balance prediction efficiency, accuracy and physical fidelity. PINN embeds physical governing equations into neural networks in the form of loss functions to integrate data rules and physical mechanisms. It has been widely adopted in fluid mechanics, solid mechanics, heat conduction and other fields, showing remarkable advantages in scenarios such as thermal conductivity inversion of composite materials and sparse temperature field reconstruction [5].

Targeting the multi-material and multi-physics coupled thermal characteristics of lithium battery modules, this paper systematically constructs a PINN theoretical framework for three-dimensional transient thermal field prediction, focuses on solving the integrated modeling problem of multi-physics mechanisms and neural networks, clarifies the physical constraint forms, network architecture design and composite loss function, and analyzes the technical advantages and application challenges of the proposed method.

II. BASIC PRINCIPLES OF PINN

The theoretical foundation of PINN originates from the universal approximation theorem, which indicates that neural networks are capable of approximating any continuous function, providing theoretical guarantee for solving partial differential equations (PDEs) via neural networks . On this basis, PINN converts PDE solving into an optimization problem of neural network parameters by constructing loss functions containing physical residuals.

2.1 Core Idea of PINN

The core innovation of PINN lies in physics-embedded modeling. A deep neural network is adopted to approximate the physical quantity to be solved, and partial differential equations (PDEs), boundary conditions (BC) and initial conditions (IC) describing the operating laws of the system are transformed into loss function constraints, guiding the network to strictly follow physical operating mechanisms while fitting measured data. Specifically, the general form of governing equations for any physical system is[6]:

$$\mathcal{N}[\mathcal{U}(x,t);\lambda] = f(x,t), \quad x \in \Omega, t \in [0,T] \qquad (1)$$

where $\mathcal{U}(x,t)$ denotes the quantity to be solved; x,t represent spatial coordinates and time variables respectively; Ω is the solution domain; $\mathcal{N}[\cdot]$stands for the nonlinear differential operator; λ refers to physical parameters of the system; $f(x,t)$is the source term.

PINN takes Multi-Layer Perceptron (MLP) as the surrogate model to approximate the physical quantity to be solved, outputting the predicted solution $\hat{u}(x,t,W,b)$, where (W,b) are network weights and biases respectively. The spatial-temporal partial derivatives of each order are calculated via automatic differentiation for the network-predicted solution, which are substituted into the differential operator $\mathcal{N}[\cdot;\lambda]$ with physical parameters to construct PDE residuals:

$$\mathcal{R}_{PDE}(x,t) = \mathcal{N}[\hat{u}(x,t,W,b);\lambda] - f(x,t) \qquad (2)$$

During the training phase, the mean square losses of PDE residuals, initial value losses and boundary condition losses are minimized simultaneously, and network parameters are updated iteratively via gradient descent. The model prediction results are constrained to satisfy governing equations and definite solution conditions, realizing the deep integration of physical prior knowledge and deep learning.

2.2 PINN Network Architecture

The backbone network of PINN generally adopts a standard fully connected feedforward neural network (FCNN), also known as Multi-Layer Perceptron (MLP). It consists of three hierarchical structures: input layer, hidden layers and output layer[7]. The input layer takes spatial-temporal coordinates(t,x,y,z) as input variables to build the mapping from continuous coordinates to physical quantities, differing from discrete solving methods based on grid modeling. Hidden layers are composed of multi-layer fully connected neurons equipped with nonlinear activation functions such as tanh and swish to fit complex nonlinear physical relationships. The output layer outputs physical quantities to be solved; single physical field solving scenarios output a single variable, while multi-physics coupling scenarios can synchronously output multiple

physical parameters. Each layer of the neural network contains multiple neurons, and each neuron is connected to all neurons of the previous layer with different weight values assigned to each connection. As shown in Figure 1, PINN realizes deep integration of physical laws and data-driven modeling through the cycle of neural network forward propagation, residual calculation via automatic differentiation, loss function construction and backpropagation optimization.

2.3 Composition of Composite Loss Function

PINN realizes dual constraints through weighted composite loss functions, and the total loss function consists of four components: physical equation residual loss, boundary condition loss, initial condition loss and data fitting loss, whose expression is[8]:

$$\mathcal{L}_{total} = w_{PDE} \cdot \mathcal{L}_{PDE} + w_{BC} \cdot \mathcal{L}_{BC} + w_{IC} \cdot \mathcal{L}_{IC} + w_{Date} \cdot \mathcal{L}_{Date} \quad (3)$$

where w_{PDE}、w_{BC}、w_{IC}、w_{Date} are weight coefficients of each loss term, used to balance the magnitude differences of different constraint items and equalize the proportion of each condition during training.

Physical equation residual loss serves as the core constraint of PINN. Collocation points are randomly sampled within the solution domain to calculate the mean square error of residuals, ensuring the physical rationality of full-domain solutions:

$$\mathcal{L}_{PDE} = \frac{1}{N_{PDE}} \sum_{i=1}^{N_{PDE}} \|\mathcal{R}_{PDE}(x_i, t_i)\|^2 \quad (4)$$

Boundary condition loss and initial condition loss are respectively adopted to constrain boundary states of the solution domain and initial states of the system, guaranteeing the integrity of model solving. Data fitting loss fits sparse measured data to build a bridge between the model and actual working conditions, acting as the core constraint for field reconstruction under sparse data scenarios.

2.4 Automatic Differentiation and Network Optimization Mechanism

A key technology of the PINN framework is Automatic Differentiation (AD). When calculating the physical equation residual $\mathcal{R}_{PDE}$, it is necessary to compute partial derivatives of the network output $\hat{u}$ with respect to input (x, t), such as $\frac{\partial \hat{u}}{\partial t}$, $\frac{\partial \hat{u}}{\partial x}$, $\frac{\partial^2 \hat{u}}{\partial x^2}$, etc. Since the neural network itself is a complex function composed of basic operations (addition, multiplication, activation functions), AD technology can accurately and analytically calculate the values of these derivatives using the chain rule, without adopting numerical difference methods with truncation errors[9]. Mainstream deep learning frameworks (e.g., TensorFlow, PyTorch) are equipped with efficient built-in AD functions.

Once the total loss function $\mathcal{L}_{total}$ and its gradient with respect to network parameters (W, b) are calculated, standard gradient descent optimization algorithms can be applied to backpropagate errors and iteratively update network parameters until the total loss converges to a sufficiently small value. At this time, the trained neural network $\hat{u}(x, t, W, b)$ becomes a continuous and differentiable approximate solution to the original PDE problem.

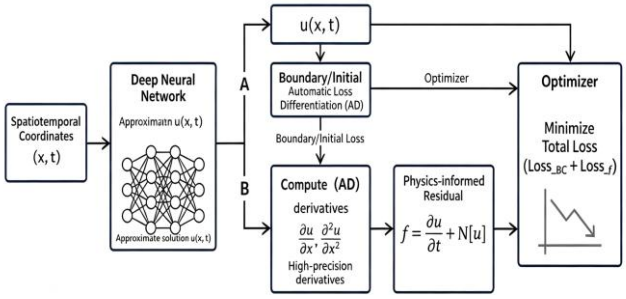

Fig. 1: diagram of the basic framework of PINN

III. CONSTRUCTION OF PINN FRAMEWORK FOR THERMAL FIELD PREDICTION OF LITHIUM BATTERY MODULES

3.1 Thermal Physical Model of Lithium Battery Module

The primary and most critical step to construct the PINN framework is establishing an accurate physical model describing system behavior. For lithium battery modules, the core is the three-dimensional transient heat conduction governing equation, with refined definition of heat source terms and boundary conditions.

3.1.1 Three-Dimensional Transient Heat Conduction Governing Equation

Without considering internal fluid flow, the temperature T at any point (x, y, z) inside the lithium battery module varying with time t follows Fourier's law of heat conduction, whose partial differential equation form is[10]:

$$\rho(x) C_p(x) \frac{\partial T(x,t)}{\partial t} = \nabla \cdot [k(x) \nabla T(x,t)] + Q_{gen}(x,t) \quad (5)$$

where $\rho(x)$ denotes material density; $C_p(x)$ represents material specific heat capacity; $k(x)$ is anisotropic thermal conductivity; $T(x, t)$ refers to the spatial-temporal temperature field; $Q_{gen}(x, t)$ is volumetric heat generation rate. For a module composed of cells, busbars, cooling

plates, thermal insulation materials and other components, the physical parameters ρ , C_p ,k are spatially inhomogeneous.

3.1.2 Coupled Heat Source Model

Heat generation inside batteries is the core driving factor of temperature variation. Traditional models often adopt simplified Bernardi mathematical models, yet more refined decomposition of heat source terms is required to improve prediction accuracy under various working conditions and temperatures. The total heat source Q_{gen} of batteries mainly consists of irreversible heat source and reversible heat source.

Temperature variation of batteries relies on heat generation[11], and heat generation rate exerts a vital influence on temperature. From the perspective of first principles, heat generation inside batteries involves complex chemical processes including irreversible heat, reversible heat, entropy change heat and multiple other types[12]. The widely adopted heat generation model is as follows :

$$Q_{Joule} = I(U - OCV) - IT\frac{\partial OCV}{\partial T} \tag{6}$$

where I represents the current passing through the battery (negative for charging, positive for discharging); U is the terminal voltage of the battery; OCV denotes open-circuit voltage. The term $(V - OCV)$ stands for total overpotential, and $\frac{\partial OCV}{\partial T}$ is the entropy heat coefficient. These electrical quantities (I, V, OCV) are generally functions of time t and State of Charge (SOC), while SOC itself is the integral result of current over time. The first term on the right-hand side of the formula represents irreversible heat generated by internal resistance and polarization resistance of the battery, and the second term refers to reversible heat induced by entropy change of battery chemical reactions. In general, the proportion of reversible heat is negligible when batteries are charged and discharged at high rates. Therefore, the final heat generation model is simplified as[13]:

$$Q_{Joule} = I(U - OCV) \tag{7}$$

From the perspective of thermodynamics and dynamics, heat generation rate defines internal heat generation of batteries and imposes a significant impact on temperature. Hence, it should be taken as an additional input feature to achieve more accurate temperature prediction for batteries.

3.1.3 Boundary and Initial Conditions

A complete description of physical problems cannot be separated from boundary and initial conditions. Initial Condition (IC): The temperature distribution of the module at the initial moment (t=0) is known. In most cases, the initial temperature can be assumed as uniform ambient temperature T_{amb} . Boundary Condition (BC): Heat exchange occurs between the outer surface of the module and the external environment, generally described via the third-type boundary condition (convective heat transfer) and fourth-type boundary condition (radiant heat transfer).

Convective heat transfer: Heat exchange between the module surface and air or cooling fluid (air cooling or liquid cooling) follows Newton's law of cooling:

$$-k(x_s)\frac{\partial T}{\partial n}\Big|_{x_s} = h(x_s)\big[T(x_s, t) - T_f(t)\big] \tag{8}$$

where x_s denotes points on the boundary surface; $\frac{\partial T}{\partial n}$ is the temperature gradient along the outward normal direction; $h(x_s)$ represents surface heat transfer coefficient (may differ at different surface positions); $T_f(t)$ is the temperature of cooling fluid.

Radiant heat transfer: Radiant heat exchange between the module surface and other objects (e.g., battery box) follows the Stefan-Boltzmann law:

$$-k(x_s)\frac{\partial T}{\partial n}\Big|_{x_s} = \varepsilon\sigma[T(x_s, t)^4 - T_{surr}(t)^4] \tag{9}$$

where ε is surface emissivity; σ stands for the Stefan-Boltzmann constant; $T_{surr}(t)$ refers to the effective radiant temperature of the surrounding environment. In engineering practice, the radiation term can sometimes be linearized and incorporated into an equivalent heat transfer coefficient if the temperature difference is small.

3.2 Design of Multi-Physics Enhanced Constraint Loss Function

To adapt to the multi-material and multi-physics coupling characteristics of lithium battery modules, charge consistency loss and interface continuity loss are newly added on the basis of traditional PINN loss functions in this paper, constructing a six-dimensional composite loss function:

$$\mathcal{L}_{total} = w_{PDE} \cdot \mathcal{L}_{PDE} + w_{BC} \cdot \mathcal{L}_{BC} + w_{IC} \cdot \mathcal{L}_{IC} + w_{Date} \cdot \mathcal{L}_{Date} + w_{ch} \cdot \mathcal{L}_{ch} + w_{in} \cdot \mathcal{L}_{in} \tag{10}$$

Basic constraints include heat conduction equation residual loss, boundary/initial condition loss and sparse data fitting loss, realizing basic physical laws of thermal fields and fitting constraints of measured data. Heat conduction residual loss constructs the mean square error of heat transfer equation residuals by solving spatial-temporal partial derivatives of temperature via automatic differentiation; boundary and initial losses constrain boundary heat exchange states and initial temperature distribution of the system; data fitting loss takes sparse

measured data from sensors as anchor points to correct model prediction deviations.

Introducing electrochemical process constraints into the lithium battery thermal model can significantly improve model performance. For this purpose, a charge consistency constraint is proposed. The PINN network is extended to simultaneously predict temperature and cumulative charge quantity.

Lithium battery modules are typical multi-material composite structures. At contact interfaces of different materials (e.g., cell and cooling plate, cell and thermal insulation pad), temperature and normal heat flux density must satisfy continuity conditions. Ignoring this will lead to physically unrealistic temperature jumps or heat flux interruptions.

IV. RESULTS AND DISCUSSION

4.1Analysis of Improved Composite Loss Constraint Mechanism

Conventional standard PINN only contains four loss components: heat conduction PDE residual loss, boundary condition loss, initial condition loss, and measurement data fitting loss. Targeting the multi-material and electro-thermal coupling characteristics of lithium-ion battery modules, this paper innovatively adds material interface continuity loss and charge consistency loss to construct a six-component composite loss function, which theoretically improves the physical constraint system of the model.

In terms of material interface constraints, lithium-ion battery modules are coupled structures composed of multi-layer heterogeneous materials, where the thermal physical parameters of cells, thermal conductive gaskets, liquid cooling plates and thermal insulation materials differ significantly. If only basic heat conduction equations are adopted for constraints, the neural network lacks mandatory restrictions at the interfaces of different materials, which tends to produce unphysical temperature jumps and heat flux interruptions that violate energy conservation and damage the physical continuity of the full-domain temperature field. After introducing the interface continuity loss, the model simultaneously enforces two constraints of temperature continuity and normal heat flux continuity at all material contact interfaces. From the perspective of loss function, this term avoids unphysical field distortion under multi-material structures and improves the physical self-consistency of full-domain temperature solution.

From the perspective of electro-thermal coupling constraints, conventional thermal PINNs only take spatial-temporal coordinates as network inputs, decoupling the inherent correlation between battery heat generation, current, state of charge (SOC) and open-circuit voltage. The heat source term is merely substituted as a fixed external load, failing to reflect the real-time variation law of heat generation during dynamic charge and discharge. This paper expands the network output variables to simultaneously solve temperature and cumulative charge capacity. The charge consistency loss restricts the integral relationship among current, SOC and heat generation, linking Joule irreversible heat and entropic reversible heat to the electrical operating conditions of batteries. Joint constraints of electrochemical and heat transfer equations are therefore realized, making up for the electro-thermal decoupling defect caused by single temperature field modeling. The heat source term can be dynamically updated with real-time operating conditions to meet the demand for temperature prediction under variable-current cycling conditions.

The composite loss function covers six types of physical constraints, and the numerical magnitudes of each loss term differ greatly during training. Fixed equal weights will render some newly added constraints ineffective. Accordingly, a phased weight optimization strategy is adopted in this framework: in the early training stage, the weights of heat conduction PDE residual loss and measurement data fitting loss are increased to enable the network to quickly learn the overall heat transfer trend; in the middle and late training stages, the weights of interface constraint loss and charge consistency loss are elevated to strengthen multi-physics auxiliary conditions. This strategy balances the fitting accuracy of measured data and the physical compliance of full-domain PDEs, and guarantees synchronous convergence of all constraint terms.

4.2 Characteristics of Temperature Field Reconstruction under Sparse Sensors

The core engineering advantage of the proposed framework lies in its capacity to reconstruct complete three-dimensional temperature fields with only a small number of sparse temperature measurement points relying on physical prior equations. Theoretical comparative analysis with finite element method (FEM) simulation and pure data-driven neural networks is carried out in this subsection.

Pure data-driven models (e.g., BP neural networks) are trained entirely relying on massive labeled temperature samples without embedding any heat transfer physical laws. When the number of temperature sensors is drastically reduced and labeled data are scarce, the model lacks sufficient supervision information to learn the spatial distribution rule of temperature. Reasonable extrapolation cannot be realized for temperature blind zones inside the module without sensors, and extreme temperature prediction results violating heat transfer laws are easily

generated. Meanwhile, internal hotspots cannot be accurately located, leading to weak generalization performance.

Finite element numerical simulation possesses complete physical mechanisms but highly depends on mesh discretization[14]. Regardless of the number of measurement points, complete geometric modeling, mesh generation and physical parameter calibration are mandatory. The iterative solving process for a single operating condition is cumbersome and time-consuming, which hardly satisfies the requirements of real-time online prediction for vehicle battery management systems (BMS) and grid energy storage systems.

Different from the above two methods, PINN takes the three-dimensional transient heat conduction PDE as a global hard constraint, and sparse sensor measurement points only serve as auxiliary supervision conditions. Physical equations compensate for the deficiency of measurement data. Automatic differentiation is adopted to solve full-domain temperature gradients, achieving continuous temperature extrapolation for blind zones without sensors such as gaps between cells, bottom surfaces of cooling plates and busbar lugs. The internal heat dissipation path and temperature gradient distribution inside the module can be fully restored without mesh modeling, which naturally adapts to practical engineering scenarios with limited sensor layout.

4.3 Adaptability Analysis under Complex Operating Conditions

The actual operation of lithium-ion batteries involves various complex working conditions including constant-rate charge/discharge, pulse variable current, low/high-temperature environments and time-varying cooling boundaries. The adaptation logic of the proposed PINN framework to various conditions is analyzed theoretically in this subsection.

For pulse dynamic charge and discharge conditions, the battery current fluctuates rapidly over time, resulting in real-time drastic variation of heat generation rate. Traditional simulation models require manual update of heat source loads at each time step, leading to tedious operation and low computational efficiency. PINNs without charge consistency loss fail to link electrical parameters, so heat source updating suffers obvious hysteresis and the tracking performance of temperature rise-fall curves is poor. The improved model in this paper binds current, SOC and heat generation terms via charge consistency constraints. Taking time as an independent input variable, the network can automatically adapt to dynamically varying volumetric heat sources and accurately capture transient temperature fluctuations.

For working conditions with time-varying heat transfer boundaries, fluctuations in liquid cooling flow rates and sharp changes in ambient temperature will cause time-dependent variations of convective heat transfer coefficients and radiative heat transfer intensity. Traditional simulations require repeated modification of boundary conditions and re-iterative calculation; the boundary loss term of the proposed model can directly constrain time-varying convective and radiative heat fluxes. Repeated geometric and boundary remodeling is unnecessary, and the framework can self-adapt to dynamic heat exchange environments.

For extreme low/high-temperature environments deviating from the optimal operating range of 20–40 ℃, material thermal conductivity, specific heat capacity and entropic heat coefficients all exhibit strong temperature dependence, introducing prominent nonlinearity into the heat conduction governing equation. Pure data models trained under room-temperature samples fail severely when extrapolated to low or high temperatures. In contrast, PINN directly incorporates temperature-dependent physical parameters into PDE residual calculation, and heat transfer equations constrain nonlinear heat transfer relations, broadening the applicable temperature range of the model.

4.4Theoretical Comparison of Computational Efficiency with Traditional Numerical Simulation

The finite element method belongs to a discrete mesh-based numerical solution. Its computational cost rises exponentially with the increase of cell quantity, mesh refinement and extension of prediction duration. Transient temperature field solving for a large-scale battery pack is extremely time-consuming and cannot support real-time online prediction.

The mesh-free PINN proposed in this paper consists of two stages: offline training and online inference. The offline stage requires collocation point sampling, PDE residual calculation and backpropagation iteration to optimize network parameters, which brings certain training overhead. Nevertheless, once training is completed, the trained network can output temperature values at any spatial-temporal coordinate through only one forward propagation, achieving millisecond-level inference speed. For long-term online monitoring scenarios of new energy vehicles and energy storage power stations, one-time training can be reused for rapid calculation under multiple similar operating conditions, presenting remarkable efficiency advantages over repeated FEM simulations. Therefore, PINN is suitable as a surrogate model to replace traditional numerical simulation.

4.5 Discussion on Model Application Bottlenecks and Internal Mechanisms

Although the multi-physics constrained PINN shows prominent advantages in physical consistency and sparse data adaptability, inherent algorithmic characteristics restrict its large-scale engineering implementation. The internal inducing mechanisms of major bottlenecks are analyzed theoretically as follows:

First, the four-dimensional spatial-temporal solution domain brings heavy computational burden during training[15]. The solution domain comprises three spatial dimensions plus one temporal dimension. A large number of internal random collocation points need to be sampled in each training iteration to guarantee effective PDE residual constraints over the full domain. With the expansion of module geometric size and prediction time window, the scale of collocation points surges, which drastically increases the computational volume of automatic differentiation. Meanwhile, gradients in high-dimensional space suffer severe instability, easily triggering gradient vanishing or gradient explosion and slowing down loss convergence.

Second, non-convex optimization challenges induced by the composite loss function. The total loss function formed by weighted superposition of six constraint terms is a typical non-convex optimization objective, so network training tends to converge to local optima rather than the global optimum. This problem becomes more severe under mismatched weights of each loss term or improper network initialization parameters. A typical failure mode is that the model fits sparse sensor temperatures well while PDE residual loss remains at a high level; predicted temperature curves match measured data but violate fundamental heat transfer laws, significantly reducing model reliability.

Third, difficulties in balancing multi-scale electro-thermal coupling constraints. Lithium-ion battery systems feature multi-scale characteristics: the microscopic scale of internal electrochemical reactions inside single cells and the macroscopic heat dissipation scale of the whole module differ by several orders of magnitude. The coupled PDE system formed by electrochemistry and heat transfer possesses strong stiffness. Simple adjustment of loss weights cannot balance the convergence rate of microscopic and macroscopic residuals, greatly increasing the difficulty of hyperparameter tuning and training iteration.

Fourth, insufficient generalization capacity under drastic structural changes. The current framework is constructed for battery modules with fixed cell stacking layout and fixed material composition. If the number of cells, cooling structure layout or material types are drastically altered, the prediction accuracy of the pre-trained network will decline obviously, requiring resampling of data and retraining. Subsequent research can introduce geometric encoding and material parameter embedding modules into the network input layer to further improve the model's universality.

V. CONCLUSIONS

This paper systematically proposes and constructs a theoretical research framework for thermal field prediction of lithium battery modules based on Physics-Informed Neural Networks (PINN). Aiming to resolve the inherent contradictions of traditional methods in computational efficiency, data dependence and physical fidelity, this framework focuses on high-precision thermal field reconstruction under sparse data conditions. Through in-depth analysis, the tremendous potential of this theoretical framework in terms of data efficiency, physical consistency, adaptability to complex problems and parameter inversion is clarified. Meanwhile, severe challenges in multi-scale coupling, high-dimensional computation, training stability and other aspects are honestly pointed out. Although this paper is limited to pure theoretical research without providing numerical results, its value lies in systematically depicting how PINN, a powerful scientific computing tool, can be applied to the critical engineering field of battery thermal management.

ACKNOWLEDGEMENTS

This work was supported by the Research Funding of GDUPT. "Research on Heat Transfer Enhancement of Heat Sink by Inverse Calculation Design Method" (No. 2019rc074).

REFERENCES

[1] Zhou, X. (2024). Research on thermal runaway detection and thermal management strategy of power battery packs for new energy vehicles. Special Purpose Vehicle, (12), 116–118

[2] Murugan, M., Elumalai, P. V., Vijayakumar, K. C. K., Babu, M., Suresh Kumar, K., Ganesh, M., ... & Prabhakar, S. (2025). A comprehensive review of thermal management methods and ideal system design for improved electric vehicle battery pack performance and safety. Energy Science & Engineering, 13(3), 1011-1036

[3] Pang, H., Wu, L., Liu, J., Liu, X., & Liu, K. (2023). Physics-informed neural network approach for heat generation rate estimation of lithium-ion battery under various driving conditions. Journal of energy chemistry, 78, 1-12

[4] Xue, K., Zhang, Z. G., Wang, Y. H., Yuan, Q. Y., Huang, T. Y., Du, X., ... & Zhang, B. (2026). Research on temperature prediction of lithium-ion batteries based on physics-informed

neural networks. Chinese Journal of Engineering, 48(4), 929–938

[5] Lyu, Y. H., Liu, Y. D., Yan, Y. J., Cai, J. F., & Huang, X. B. (2026). Inversion method for equivalent thermal conductivity of bushing capacitor core based on physics-informed neural networks. Transactions of China Electrotechnical Society

[6] Raissi, M., Perdikaris, P., & Karniadakis, G. E. (2018). Physics-informed neural networks: A deep learning framework for solving forward and inverse problems involving nonlinear partial differential equations. Journal of Computational physics, 378(C)

[7] Ge, M. Y., & Li, K. F. (2025). Research on solving model of nonlinear differential equations based on physics-informed neural networks. Information Technology and Informatization, (10), 121–124

[8] Yan, C., & Yan, H. (2025). A physics-informed neural network based on stage-adaptive resampling. Acta Mechanica Sinica

[9] Halim, M. A. S., & Hoe, T. T. (2024). Introduction to Automatic Differentiation and Neural Differentiation Equation. Proceedings of Science and Mathematics. Universiti Teknologi Malaysia

[10] Kakaç, S., Yener, Y., & Naveira-Cotta, C. P. (2018). Heat conduction. CRC press

[11] Bernardi, D., Pawlikowski, E., & Newman, J. (1985). A general energy balance for battery systems. Journal of the electrochemical society, 132(1), 5-12

[12] Xue, K., Zhang, Z. G., Wang, Y. H., Yuan, Q. Y., Huang, T. Y., Du, X., ... & Zhang, B. (2026). Research on temperature prediction of lithium-ion batteries based on physics-informed neural networks. Chinese Journal of Engineering, 48(4), 929–938

[13] Chen, L. E., Zeng, X. Y., Zeng, Z. H., Cheng, C. C., & Sun, Y. K. (2024). Lithium-ion battery temperature prediction combining physical information and deep neural networks. Electric Power, 57(11), 18–25

[14] Yoon, K., Kim, J., Pyeon, H., Kim, K., & Han, S. (2024, October). Physics-informed neural network for heat transfer problem with cylindrical heat sources in battery pack geometry. In 2024 24th International Conference on Control, Automation and Systems (ICCAS) (pp. 702-705). IEEE

[15] Jeong, M., Seo, G., & Hwang, E. (2026). Mitigating Instability in High Residual Adaptive Sampling for PINNs via Langevin Dynamics. Advances in Neural Information Processing Systems, 38, 121574-121620